

Synthesis and Fluorescence Sensing for Nitro Explosives and Pesticides of Two Cd-Coordination Polymers

Hua-li Cui,* Wen Liu, Xin-yue Xu, Jie Zhou, Xiao-ming Song, and Xiao-li Chen

Cite This: *ACS Omega* 2023, 8, 39917–39927

Read Online

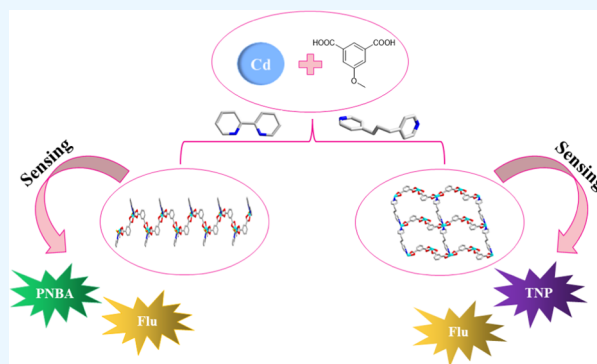
ACCESS |

Metrics & More

Article Recommendations

Supporting Information

ABSTRACT: Two cadmium coordination polymers (CPs), $\{[\text{Cd}(\text{zgt})(2,2'\text{-bipy})(\text{H}_2\text{O})]\cdot\text{H}_2\text{O}\}_n$ (1) and $\{[\text{Cd}(\text{zgt})(\text{BPP})(\text{H}_2\text{O})]\cdot\text{H}_2\text{O}\}_n$ (2) (H_2zgt = 5-methoxyresorcinic acid, 2,2'-bipy = 2,2'-bipyridine, and BPP = 1,3-bis(4-pyridyl)propane), were prepared by the hydrothermal method. The structures of CPs 1–2 were characterized by IR, TGA, X-ray powder diffraction, and elemental analysis. The single-crystal structure analysis shows that CP 1 is a typical 1D chain structure and CP 2 belongs to a 2D layered structure. Based on the excellent luminescence properties of CP 1 and 2, fluorescence sensing experiments were carried out for explosives and pesticides. The results of the explosion sensing experiment showed that CP 1 and 2 had an excellent fluorescence quenching effect on PNBA (p-nitrobenzoic acid) and TNP (2,4,6-trinitrophenol), respectively, and the detection limits were 3.28 and 11.4 nM, respectively. Interestingly, both CP 1 and 2 showed good fluorescence quenching against the pesticide fluridone (Flu), and CP 1 had a lower detection limit and was more sensitive. In addition, the fluorescence quenching mechanism was discussed in detail by the UV absorption spectrum and density functional theory. In order to explore its practical application, the content of Flu in water samples was detected by a labeling recovery method.



1. INTRODUCTION

With the progress of modern society and the rapid development of industry, the common pollutants in water such as heavy metal ions,^{1–3} organic matter,^{4–6} pesticides,^{7–9} and antibiotics^{10–12} pose a certain threat to human health. Water pollution has gradually become an intractable problem faced by people in today's society, so the detection of pollutants in water is particularly necessary. Researchers have tried a variety of detection methods, such as electrochemical methods, inductively coupled plasma atomic emission spectrometry (ICP-AES), high-performance liquid chromatography (HPLC), atomic absorption spectrometry (AAS), or mass spectrometry (MS). However, these methods have shortcomings such as complex instrument operation, high cost, long time, and insensitivity, so researchers are urgently looking for a simple and responsive detection technology, and the photochemical method is regarded as an effective detection method because of its low cost, high sensitivity, and selectivity.

There are pesticide residues on crops, and there are many ways in which pesticides can be present in our food and drinking water and threaten our health, so pesticide detection is tricky. Nitrocellulose explosive,^{13–15} a common chemical raw material, is an explosive and toxic substance, which can pollute groundwater and soil and harm people's health. The fluorescence method^{16–20} can detect explosives quickly and efficiently. Therefore, it is very necessary to establish a kind of

fluorescence sensor that can detect both pesticides and nitro explosives.

Luminescent sensing materials are attractive for environmental analysis due to their high selectivity, excellent sensitivity, and potential for rapid (even instantaneous) response to target analytes in different sample matrices.²¹ Many types of analytes have been detected in wastewater samples used for environmental protection, reagents and products used in pharmaceutical and pesticide industrial production, and biomarkers in blood and urine used for early diagnosis. However, developing suitable materials with the best sensing function for the target analyte remains challenging.^{22,23} Coordination polymers (CPs)^{24–26} are a class of porous materials formed by the coordination of metal and organic ligands. They have the characteristics of rich and varied structure, large specific surface area, adjustable aperture, and good luminescence performance. Due to their unique and excellent luminescence characteristics, they are often widely used as luminous sensors in the field of fluorescence analysis.²⁷ It is still a challenge to design and synthesize

Received: August 28, 2023

Accepted: October 3, 2023

Published: October 16, 2023



luminous CP materials with high sensitivity and selectivity for the detection of pollutants in water. Therefore, the establishment of convenient and efficient complex fluorescence sensors for water pollution has become a research hotspot.

Liu et al.²⁸ synthesized a light-emitting 3D supramolecular Cd-CP that can selectively detect TNP in 13 electron-deficient explosives with a detection limit of 0.27 μM . Fluorescence quenching can be explained by a combination of fluorescence resonance energy transfer (FRET) and photoinduced electron transfer (PET). Chen et al.²⁹ synthesized six kinds of Cd-coordination polymers by the hydrothermal method, and their fluorescence responses to Fe^{3+} , anions, aspartic acid, and bovine serum albumin were studied. The research results indicate that the complex has a low detection limit for the responsive compound, indicating that Cd-MOFs have great potential in fluorescence detection. Bairy et al.³⁰ and Liu et al.³¹ also synthesized some Cd-MOFs and conducted experiments to study their properties, achieving good results, indicating that Cd-MOFs have good application prospects in the future. This also proves the correctness of our work direction. Li et al.³² synthesized a novel 3D Eu-CP by the solvothermal method. Eu-CP shows chemical stability and tolerance in water and organic solvents, and its intense fluorescence is not affected by pH (pH = 3–12). Eu-CP can rapidly detect antibiotics like metronidazole (MDZ) and dimethylimidazole (DMZ) and pesticides like 2, 6-dichloro-4-nitroaniline (DCN) in water, with good recyclability and a low detection limit. MDZ, DMZ, and DCN have been successfully detected in calf serum and lake water. Liu's team³³ synthesized one Zn-CP and three Cd-CPs to study the fluorescence properties of CPs 1–4 against explosives. The experiment showed that increasing the concentration of explosives would reduce the fluorescence intensity of CPs 1–4, especially the CPs containing TNP solution; the fluorescence intensity decreased most obviously. Through comparison, the quenching efficiency decreased in the following order: 2,4,6-trinitrophenol > p-nitrophenol > 4-nitrotoluene > nitrobenzene, which is consistent with the polarity order of the four explosives. It can be concluded that the greater the polarity of the explosives, the better the fluorescence quenching effect of the CPs.

Wang et al.³⁴ synthesized a series of highly luminous complexes based on H_2zgt : $[\text{Ln}_2(\text{mip})_3(\text{H}_2\text{O})_8 \cdot 4\text{H}_2\text{O}]_n$ (Ln = Sm, Eu, Gd, Tb, Dy). The experimental results show that weak intermetallic energy transfer can be used to predict the color modulation of heteronuclear families by adding color strategies. We synthesized complexes CP 1 and CP 2 under hydrothermal conditions using Cd metal with excellent luminescence properties, H_2zgt , and nitrogen-containing ligands.

2. EXPERIMENTAL SECTION

2.1. Materials and Methods. All reagents were commercially available and of analytical grade and used without any purification treatment. Thermogravimetric analysis (TGA) was performed using a NETZSCHSTA 449C thermogravimetric analyzer in a nitrogen atmosphere with temperature increased from room temperature to 900 $^\circ\text{C}$ at a heating rate of 10 $^\circ\text{C} \cdot \text{min}^{-1}$. The IR spectra of KBr particles in the region of 4000–400 cm^{-1} were recorded on a Bruker EQUINOX55 spectrophotometer. X-ray diffraction (XRD) was carried out on a Rigaku D/Max 3III diffractometer with Cu $K\alpha$ radiation ($\lambda = 0.15418 \text{ nm}$) from 5 to 50 $^\circ$. The UV–vis spectra were measured using a UV-2700 spectrophotometer. The fluores-

cence spectrum was determined by a F-7100 spectrometer made by Hitachi of Japan.

2.2. Synthesis of $\{[\text{Cd}(\text{zgt})(2,2'\text{-bipy})(\text{H}_2\text{O})] \cdot \text{H}_2\text{O}\}_n$ (1). Accurately weighed $\text{Cd}(\text{NO}_3)_2 \cdot 4\text{H}_2\text{O}$ (0.075 mmol, 23.1 mg), H_2zgt (0.065 mmol, 12.7 mg), and 2,2'-bipy (0.05 mmol, 7.8 mg), dissolved in *N,N*-dimethylformamide (DMF) (2 mL) and H_2O (5 mL), were transferred to 10 mL transparent glass bottles, placed in an oven at 95 $^\circ\text{C}$, and the reaction was carried out at constant temperature for 5 days to obtain a final colorless transparent massive crystal, in calculated yield of 58% based on Cd. Anal. calculated for $\text{C}_{19}\text{H}_{18}\text{CdN}_2\text{O}_7$ (%): C, 45.71; H, 3.61; N, 5.61; Measured (%): C, 45.73; H, 3.62; N, 5.59. FT-IR (KBr, cm^{-1}): 3534 (w), 3526 (m), 3117 (w), 3085 (w), 3005 (w), 2356 (w), 1803 (w), 1555 (s), 1443 (s), 1394 (s), 1363 (s), 1266 (m), 1138 (m), 1058 (s), 1018 (w), 914 (m), 777 (s), 722 (s), 649 (m), 409 (m).

2.3. Synthesis of $\{[\text{Cd}(\text{zgt})(1,3\text{-bis})(\text{H}_2\text{O})] \cdot \text{H}_2\text{O}\}_n$ (2). Accurately weighed $\text{Cd}(\text{NO}_3)_2 \cdot 4\text{H}_2\text{O}$ (0.075 mmol, 23.1 mg), H_2zgt (0.065 mmol, 12.7 mg), and 1,3-bis (0.05 mmol, 9.8 mg), dissolved in *N,N*-dimethylacetamide (DMA) (1 mL) and H_2O (5 mL), were taken. The mixture was stirred evenly and transferred to a 10 mL transparent glass bottle, placed in a hot air drying oven at 95 $^\circ\text{C}$, and the reaction was carried out at constant temperature for 5 days to obtain a final colorless transparent massive crystal, in calculated yield of 55% based on Cd. Anal. calculated for $\text{C}_{22}\text{H}_{24}\text{CdN}_2\text{O}_7$ (%): C, 48.81; H, 4.44; N, 5.18; Measured (%): C, 48.80; H, 4.42; N, 5.19. FT-IR (KBr, cm^{-1}): 3670 (w), 3374 (s), 2973 (s), 2901 (s), 1627 (s), 1562 (s), 1458 (m), 1378 (s), 1250 (m), 1058 (s), 881 (m), 802 (m), 737 (m), 609 (w), 569 (w), 504 (m), 432 (w).

2.4. X-ray Crystallography. Crystals of CPs 1–2 without cracks were selected at room temperature, X-ray diffraction was carried out using graphite-monochromatized Mo $K\alpha$ radiation ($\lambda = 0.071073 \text{ nm}$) on a Bruker APEX-II single-crystal diffractometer at 298 K, and the diffraction intensity data were collected. The diffraction intensity data were corrected using the SADABS program by semiempirical absorption. The structure was solved by direct methods using the SHELXTL-2018 program, and full matrix least-squares optimization was performed based on F^2 . The coordinates of all of the hydrogen atoms were obtained through theoretical hydrogenation. All non-hydrogen atoms were refined by anisotropic displacement parameters. The riding model was used to refine the hydrogen atom isotropic in the computational position, and its Uiso value was limited to 1.2 times the parent atomic Ueq. The disordered solvent molecules in the structure were removed by the PLATON/SQUEEZE program. The crystal parameters of CPs 1–2 are shown in Table 1, the main bond lengths and angles of CPs 1–2 are shown in Tables S1 and S3, and the hydrogen bond angles (deg) and bond distances (nm) of CP 1 are listed in Table S2. CCDC: 2219473 (1) and 2220218 (2).

2.5. Luminescence Sensing Experiments. The fluorescence induction experiments were performed at room temperature. First, 30 mg of CP 1 or CP 2 powder was finely dispersed in 100 mL of distilled water, sonicated for 1 h, and left for 24 h, and the supernatant was taken for use. Then, 20 μL of the prepared series of nitroaromatic compounds (10 mmol/L) and pesticides (10 mmol/L) were used. Nitroaromatic compounds (NACs) included 2,4-dinitrophenylhydrazine (DNPH), ortho-nitroaniline (O-NT), 2,4,6-trinitrophenylhydrazine (TRI), nitrobenzene (NB), 3-nitroaniline (3-NT), para-nitrophenylhydrazine (4-NPH), p-nitrophenol (4-NP), p-nitrobenzoic acid (PNBA), O-nitrophenol (O-NP), and 2,4,6-trinitrophenol

Table 1. Crystallography Data of CP 1 and CP 2

identification code	1	2
empirical formula	C ₁₉ H ₁₈ CdN ₂ O ₇	C ₂₂ H ₂₄ CdN ₂ O ₇
formula weight	498.75	540.83
temperature/K	296.15	296.15
crystal system	monoclinic	monoclinic
space group	<i>P</i> 2 ₁ / <i>c</i>	<i>C</i> 2/ <i>c</i>
<i>a</i> /Å	9.029(5)	16.463(5)
<i>b</i> /Å	17.450(9)	17.105(5)
<i>c</i> /Å	12.646(7)	18.809(6)
α /°	90	90
β /°	96.337(8)	109.226(5)
γ /°	90	90
<i>V</i> /Å ³	1980.1(18)	5001(3)
<i>Z</i>	4	8
ρ_{calc} (g/cm ³)	1.673	1.437
μ (mm ⁻¹)	1.147	0.914
<i>F</i> (000)	1000.0	2192.0
reflections collected	9718	16166
<i>S</i> on <i>F</i> ²	1.112	1.084
<i>R</i> ₁ , <i>wR</i> ₂ ^a [<i>I</i> > 2 σ (<i>I</i>)]	0.0260, 0.0603	0.0432, 0.1285
<i>R</i> ₁ , <i>wR</i> ₂ ^a (all data)	0.0315, 0.0627	0.0543, 0.1421

$$^a R_1 = \sum ||F_o| - |F_c|| / \sum |F_o|, wR_2 = [\sum w(F_o^2 - F_c^2)^2 / \sum w(F_o^2)^2]^{1/2}$$

(TNP). Pesticides included imazalil (Ima), pyrimethanil (Pth), emamectin benzoate (Em-B), zhongshengmycin (Myc), 2,4-epibrassinolol (24-epi), pyraclostrobin (Pst), prochloraz (Pro), triadimefon (Tdi), and fluazinam (Flu).

3. RESULTS AND DISCUSSION

3.1. Crystal Structures. According to the results of X-ray single crystal diffraction analysis, CP 1 is a monoclinic system belonging to the *P*2₁/*c* space group. Each unit contains a crystallographically independent Cd^{II} ion, a zgt²⁻ ligand, a 2,2'-bipy ligand, a coordinated water molecule, and a lattice water molecule. The central Cd^{II} ion adopts a seven-coordination mode in a twisted pentagonal dipyramidal configuration. Among the seven atoms directly coordinated with Cd1, there are five oxygen atoms (O1, O2, O3#1, O4#1, and O6) and two nitrogen atoms (N1 and N2), as shown in Figure 1a. O1, O2, O3#1, and O4#1 all come from the zgt²⁻ ion, and O6 comes from the coordination water molecule. The bond length of the Cd–O bond ranges from 2.278 (2) to 2.625 (2) Å. Both N1 and N2 are derived from 2,2'-bipy molecules, and the bond length of the Cd–N bond ranges from 2.3350 (19) to 2.344 (2) Å, which is similar to that of Cd-CP reported in the literature.

In the coordination process of H₂zgt, two protic hydrogens are removed to form zgt²⁻. zgt²⁻ adopts the coordination mode

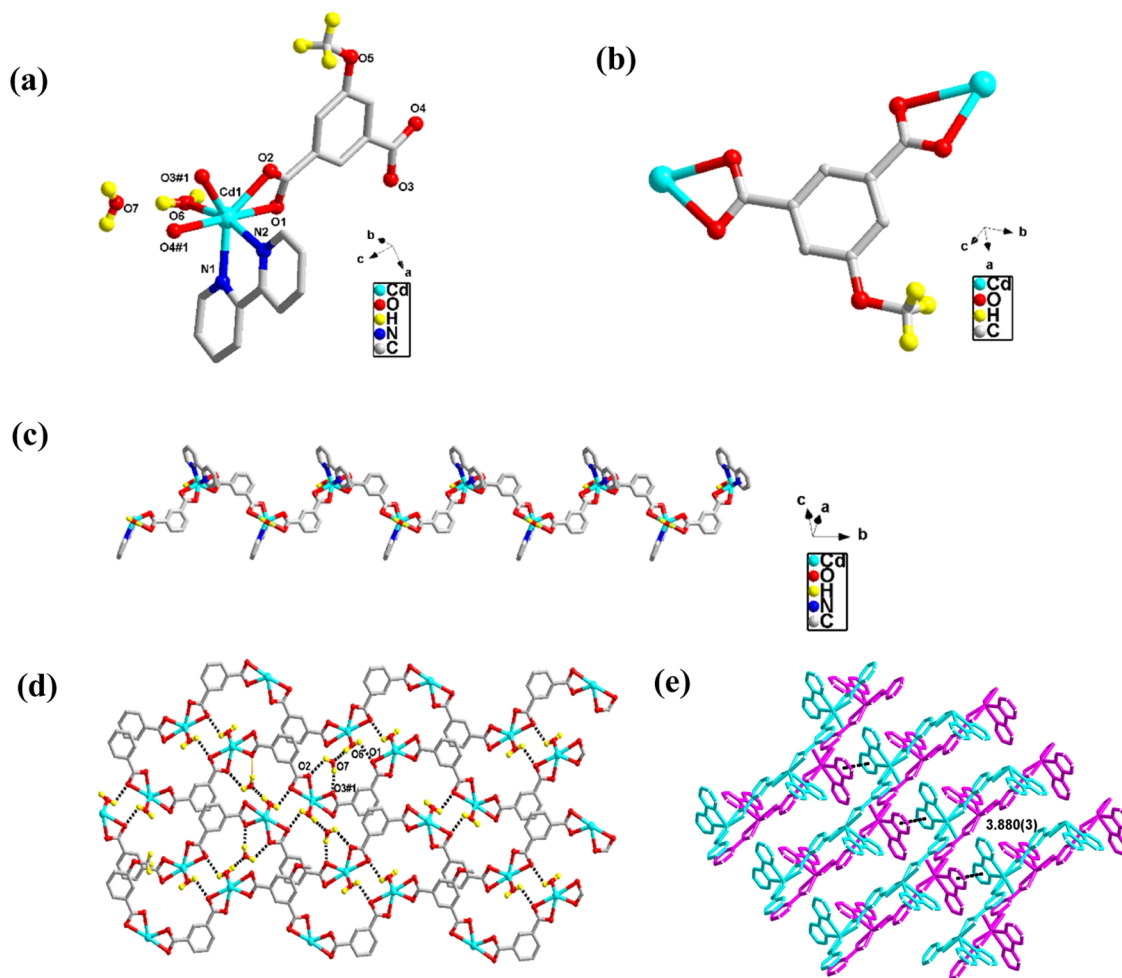


Figure 1. (a) Coordination pattern of Cd^{II} in CP 1; (b) coordination pattern of zgt²⁻ in CP 1; (c) one-dimensional chain of CP 1; (d) two-dimensional structure of CP 1, the dotted line is hydrogen bonding; and (e) three-dimensional supramolecular structure of CP 1, the dotted line is π - π packing. (Symmetry Codes: #11 - *x*, 1/2 + *y*, 1/2 - *z*).

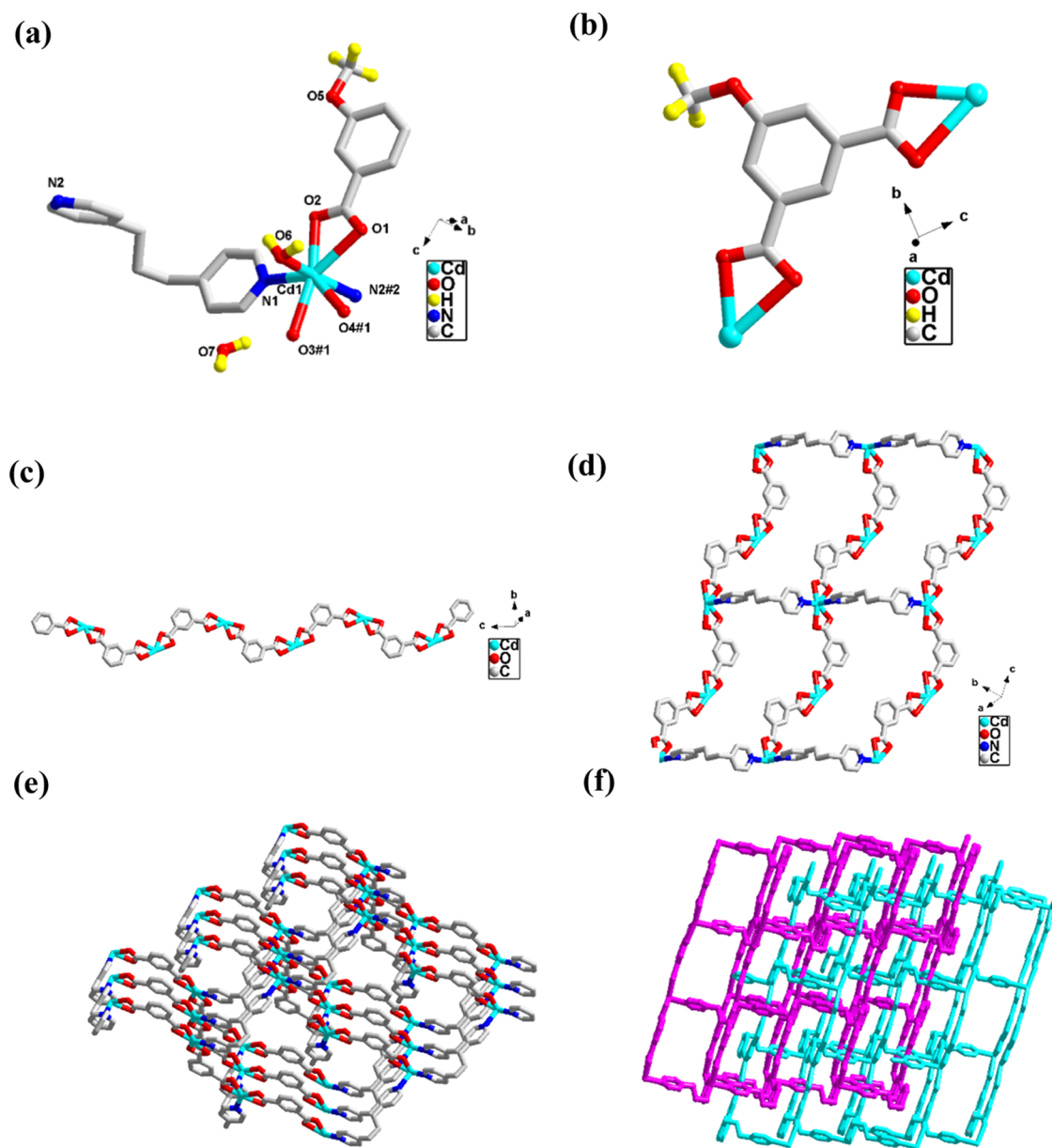


Figure 2. (a) Coordination pattern of Cd^{II} in CP 2 (symmetry codes: #1 $x, 1 - y, 1/2 + z$; #2 $1/2 + x, 1/2 + y, + z$); (b) coordination pattern of zgt^{2-} in CP 2; (c) one-dimensional chain of CP 2; (d) two-dimensional structure of CP 2; (e) single three-dimensional supramolecular structure of CP 2; and (f) three-dimensional supramolecular interpenetrating structure of CP 2.

of $\mu_2\text{-}\eta^1\text{-}\eta^1$, and both carboxylic acids are attached to the metal Cd^{II} ion by chelating bidentals, as shown in Figure 1b. Based on this coordination pattern, adjacent metals form 1D chains through zgt^{2-} ion connections (Figure 1c). The adjacent chains are linked into the 2D supramolecular network under the directions of the hydrogen bonding interaction between the lattice water molecule oxygen atom and the carboxylate group oxygen atom of [O6–H6A···O7, 2.640 (3) Å, O6–H6B···O1, 2.727 (3) Å, O7–H7A···O2, 2.889 (3) Å, O7–H7B···O3#1, 2.736 (3) Å] (Figure 1d). Then, the adjacent 2D network forms 3D supramolecular structures through $\pi\text{-}\pi$ stacking (3.880 (3) Å), as shown in Figure 1e.

CP 2 is a monoclinic system belonging to the $C2/c$ space group. Each misformation unit contains a crystallographically independent Cd^{II} ion, a zgt^{2-} ligand, a BPP ligand, and a coordination and a free water molecule (Figure 2a). The central metal Cd^{II} ion adopts a seven-coordination pattern, in which

four coordination oxygen atoms (O1, O2, O3, and O4) are derived from the zgt^{2-} ligand, another coordination oxygen atom (O6) is derived from coordination water, and two nitrogen atoms (N1 and N2) are derived from the BPP ligand. The bond length of the Cd–O bond is 2.299(3)–2.562(3) Å, and the bond length of the Cd–N bond is 2.311(3)–2.340(3) Å, which is similar to the reported value.³⁴

The zgt^{2-} ligand uses the coordination mode of $\mu_2\text{-}\eta^1\text{-}\eta^1$, and the two carboxyl groups are chelated with two Cd^{II} ions bidentately (Figure 2b). According to this coordination pattern, two adjacent metal Cd^{II} ions are connected via the zgt^{2-} ligand to form a one-dimensional chain (Figure 2c). The adjacent one-dimensional chains form a two-dimensional network structure through the connection of the BPP ligand in different directions (Figure 2d). Interestingly, the three-dimensional structure of CP 2 (Figure 2f) is formed by the interpenetration of two-

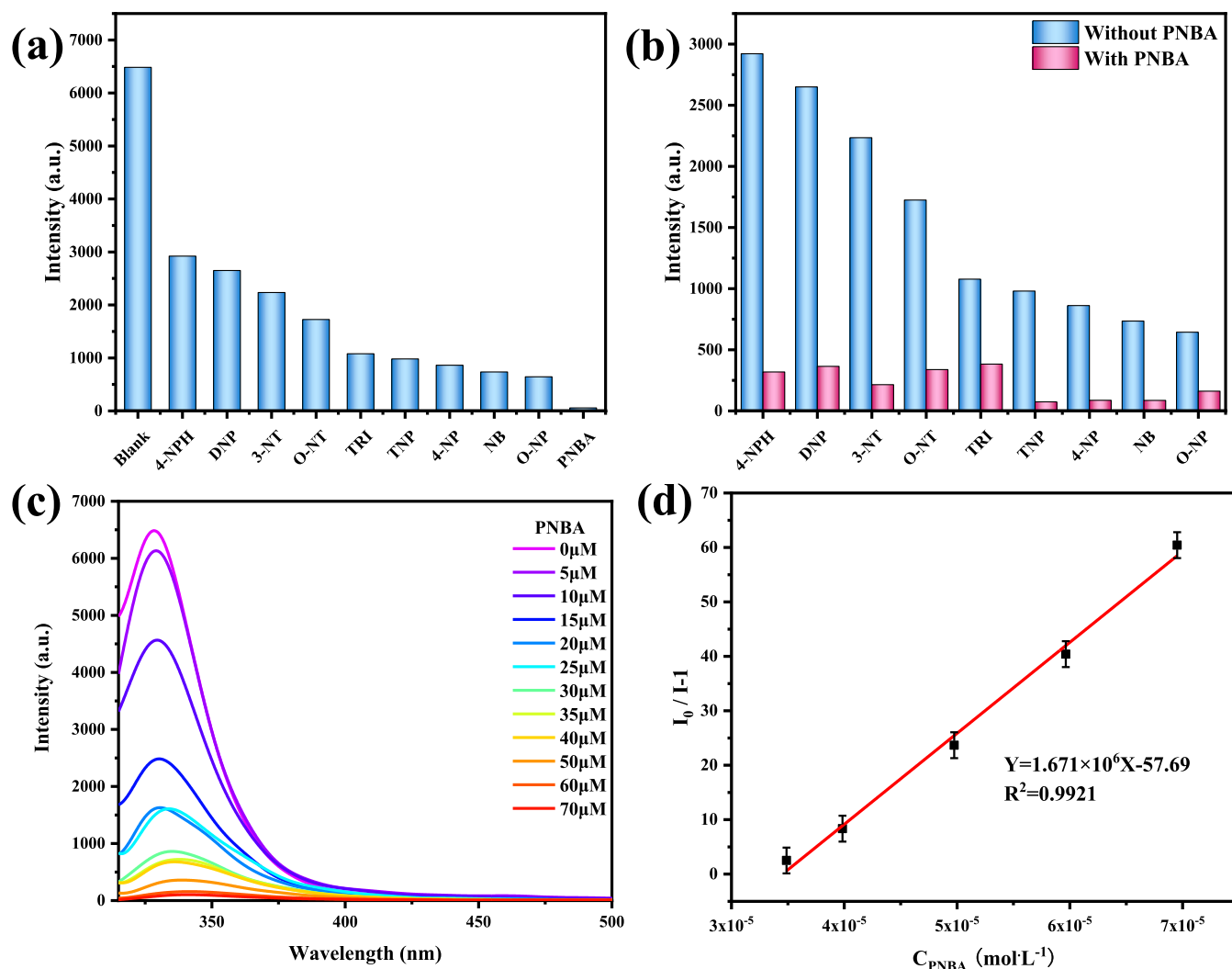


Figure 3. (a) Fluorescence intensity of CP 1 dispersed in different nitroaromatic compounds; (b) anti-interference experiment; (c) fluorescence emission spectrum of CP 1 with different concentrations of PNBA; and (d) linear fitting curve.

dimensional network structures with the same structure and different angles (Figure 2e).

3.2. Thermogravimetric Analyses. In order to be better applied in practice, the stability tests of CP 1-2 become extremely important. The thermal stabilities of CP 1-2 are tested under nitrogen protection at a heating rate of $10\text{ }^\circ\text{C}$ per minute, according to TGA spectral analysis (Figure S1). For CP 1, solvent water molecules are lost at $140\text{ }^\circ\text{C}$; the weight loss rate is 8% (calcd. 7.2%). At $230\text{ }^\circ\text{C}$, the skeleton begins to collapse. For CP 2, solvent water molecules are lost at $120\text{ }^\circ\text{C}$; the weight loss rate is 7% (calcd. 6.7%). Its skeleton begins to collapse at $210\text{ }^\circ\text{C}$. Both ultimately exist in the form of CdO. The test results indicate that all CPs have good thermal stability.

3.3. PXRD Analysis. In order to verify the purity of the synthesized complex, powder X-ray diffraction experiments were conducted on CPs 1-2, as shown in Figure S2. The experimental results show that the position and intensity of the diffraction peaks are roughly the same as the simulated data, which indicates that CPs 1-2 have good phase purity and integrity.

3.4. Solid-State Fluorescence of CPs 1-2. It has been reported that Cd-CP has excellent fluorescence properties and is often used as a fluorescence sensor to detect pollutants. Therefore, we tested the solid-state fluorescence of CPs 1-2

in order to determine whether to conduct further fluorescence sensing performance tests. The test results are known at room temperature at the same voltage and slit: CPs 1-2 (λ_{ex} 380, 356 nm), CPs 1-2 (emission peaks λ_{em} position 471 nm, 465 nm), respectively. The solid-state fluorescence of H_2zgt ($\lambda_{\text{ex}} = 385\text{ nm}$) was also detected. The position of the emission peak λ_{em} is 448 nm, as shown in Figure S3.

Compared with H_2zgt , the fluorescence intensity of CPs 1-2 was significantly enhanced, and the range was large. The emission peak position of the complex was red-shifted compared with H_2zgt , which was probably due to the charge transfer between H_2zgt and Cd^{II} ion.³⁵ In short, CPs 1-2 showed enhanced fluorescence intensity compared to ligands.

3.5. NAC Sensing. As shown in Figure 3a, fluorescence intensities of emission spectra ($\lambda_{\text{em}} = 328\text{ nm}$) of different nitro explosives ($10\text{ }\mu\text{L}$, 10 mmol/L) under excitation spectra ($\lambda_{\text{ex}} = 304\text{ nm}$) were recorded, and the fluorescence intensities of different analytes were made as bar charts, which could be clearly seen. CP 1 has different quenching effects on different nitro explosives, but the quenching effect on p-nitrobenzoic acid (PNBA) is the most obvious. In addition, it is necessary to explore whether CP 1 can still selectively detect PNBA in the presence of other nitro explosives. PNBA ($10\text{ }\mu\text{L}$, 10 mmol/L)

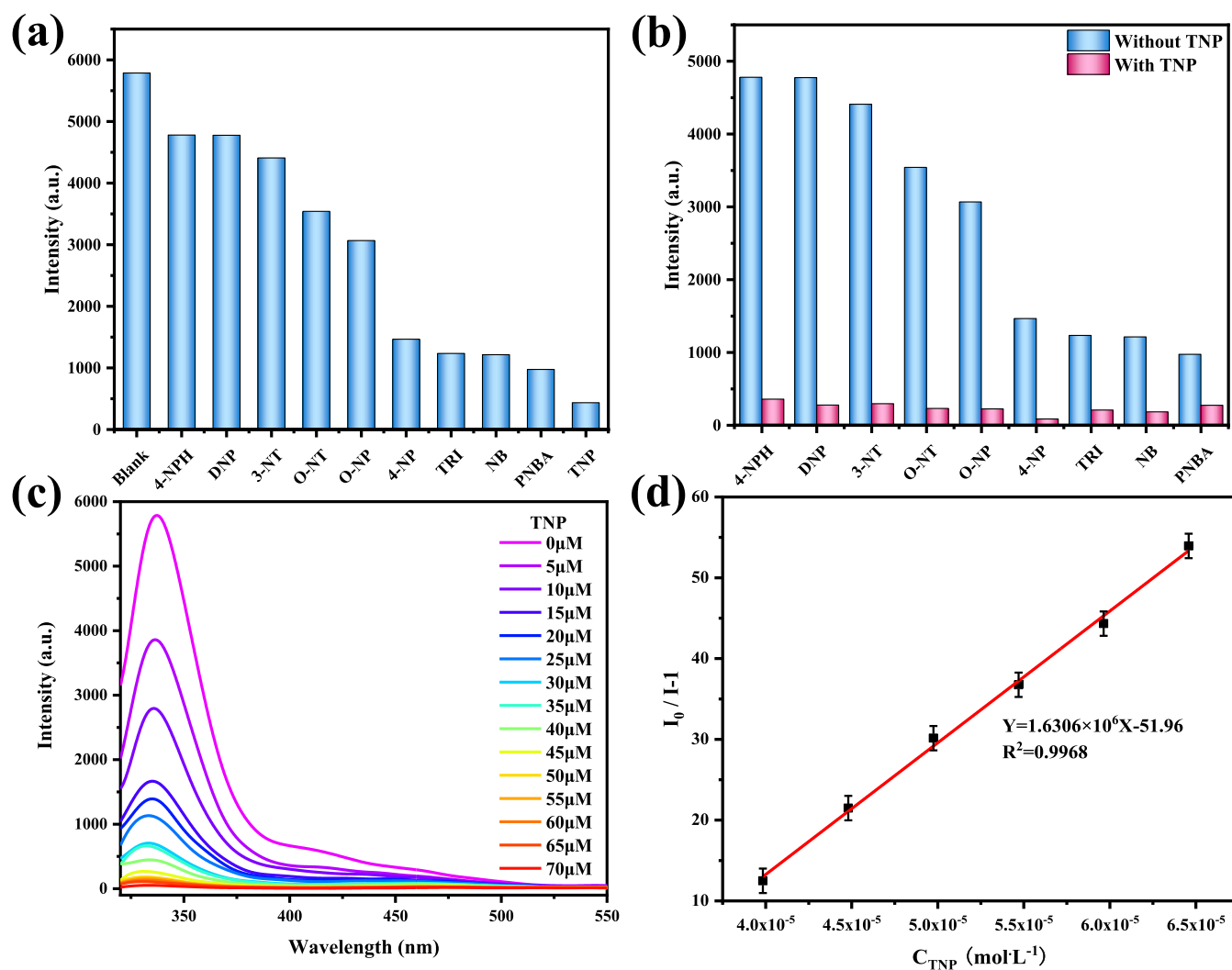


Figure 4. (a) Fluorescence intensity of CP 2 dispersed in different nitroaromatic compounds; (b) anti-interference experiment; (c) fluorescence emission spectrum of CP 2 with different concentrations of TNP; and (d) linear fitting curve.

was added into a CP 1 suspension containing other nitro explosives ($10 \mu\text{L}$, 10 mmol/L). The fluorescence intensity did not decrease sharply after the addition of other nitro explosives, but the fluorescence was almost completely quenched after the addition of equimolar amounts of PNBA, as shown in Figure 3b. The results of the anti-interference experiment show that the addition of PNBA is not interfered with by other nitro explosives, which proves that CP 1 has good selectivity to PNBA, and CP 1 has better anti-interference performance.

Based on the good quenching response of CP 1 to PNBA, a quantitative experiment was conducted to test CP 1 at room temperature, and the change rule of fluorescence intensity of CP 1 was explored by quantitatively increasing the concentration of PNBA. As the concentration of PNBA increased from 0 to $70 \mu\text{mol/L}$, the fluorescence intensity of CP 1 decreased gradually, and CP 1 was almost completely quenched when the concentration of PNBA increased to $70 \mu\text{mol/L}$, as shown in Figure 3c. In order to more accurately study the relationship between PNBA concentration and fluorescence intensity, linear fitting was carried out according to the S–V equation. When the concentration increased to $70 \mu\text{mol/L}$, the linear relationship was shown in the low concentration range (3×10^{-5} to 7×10^{-5}): $Y = 1.671 \times 10^6 X - 57.69$ ($R^2 = 0.9921$) (Figure 3d). The detection limit (LOD) can be obtained by using the equation

$\text{LOD} = 3\sigma/K$. The final detection limit reaches the nM level, and the accurate detection limit of PNBA is 3.28 nM , which is lower than the reported value^{36,37} and shows that CP 1 can detect PNBA sensitively.

The specific operation of CP 2 detection of explosives is the same as above. The emission spectra of different objects to be measured under excitation spectra ($\lambda_{\text{ex}} = 310 \text{ nm}$) are recorded respectively, and the emission peak position is at the wavelength 336 nm . Fluorescence intensity was quenched for different substances to be tested but at the same time showed different degrees of quenching; especially, the quenching effect of 2,4,6-trinitrophenol (TNP) was the most obvious (Figure 4a). In order to explore the antijamming ability of CP 2, the antijamming experiment was carried out. The experimental results are listed in Figure 4b. CP 2 is not interfered with by other tested substances and TNP, and it still has a significant quenching effect without interference from other tested substances.

Based on the above experimental results, we conducted a quantitative experiment to detect TNP with CP 2 at room temperature and studied the change rule of fluorescence intensity of CP 2 with the increase of TNP concentration. As shown in Figure 4c, the fluorescence intensity of CP 2 decreased with the increasing concentration of TNP. The fluorescence was

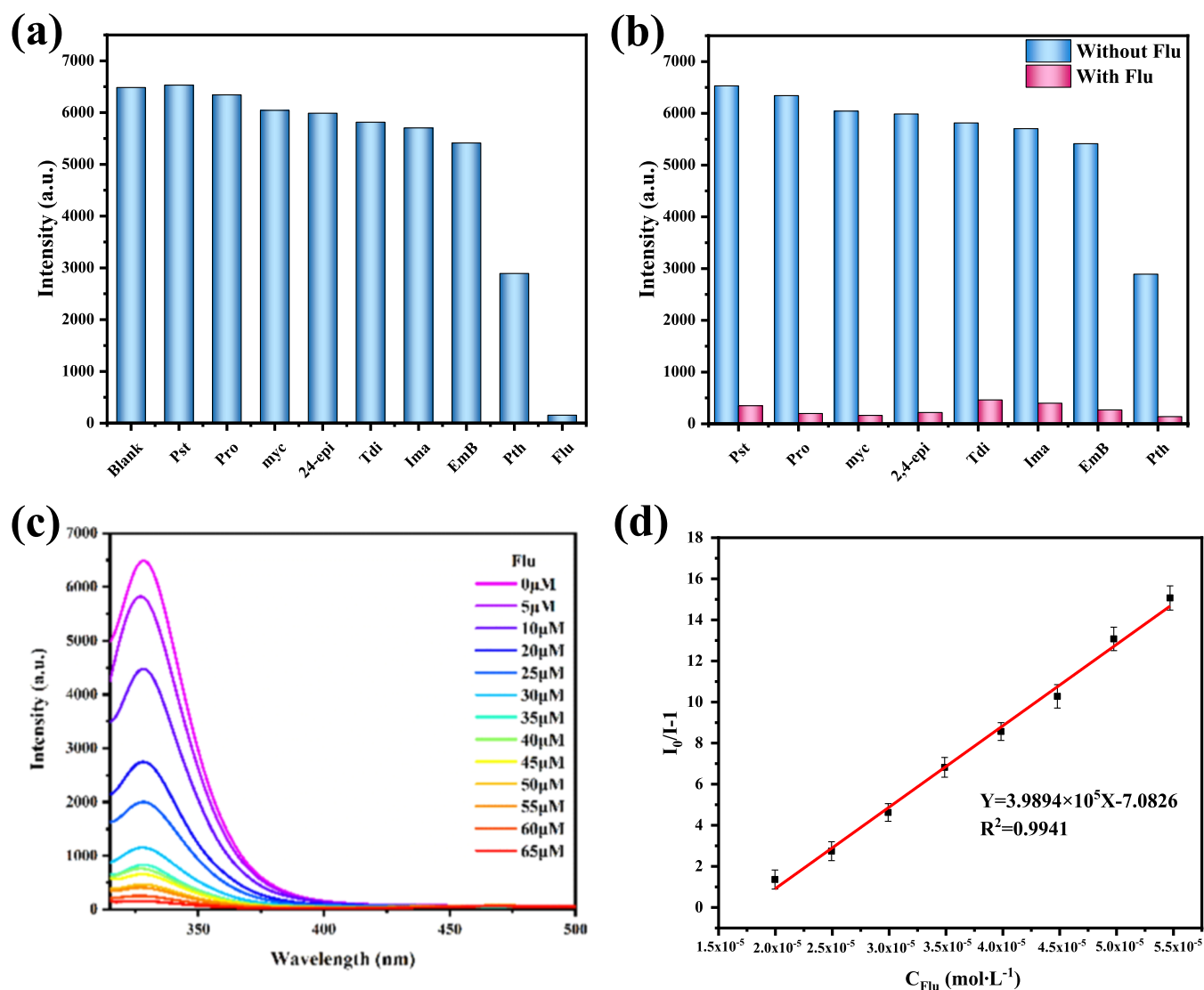


Figure 5. (a) Fluorescence intensity of CP 1 dispersed in different pesticides; (b) anti-interference experiment; (c) fluorescence emission spectrum of CP 1 with different concentrations of Flu; and (d) linear fitting curve.

almost completely quenched when the concentration of TNP increased from 0 to 70 $\mu\text{mol/L}$. The results showed that CP 2 was almost completely quenched when the concentration of TNP was increased to 70 $\mu\text{mol/L}$. In order to further study the precise relationship between the concentration of TNP and the fluorescence intensity of CP 2, linear fitting was conducted according to the S–V equation, as shown in Figure 4d. In the low concentration range, the linear relationship was good: $Y = 1.6306 \times 10^6 X - 51.96$ ($R^2 = 0.9968$), and the detection limit was 11.4 nM. The detection limit is lower than the reported value.³⁸

3.6. Pesticide Sensing. Due to the excellent luminescence performance and water stability of CPs, we evaluated their potential detection for pesticides. This measure has long-term significance for both environmental protection and human health.³⁹

When the excitation spectrum of CP 1 is 304 nm, the emission spectrum of CP 1 is 328 nm. Due to the pore structure and excellent fluorescence properties of CP 1, the potential of CP 1 as a pesticide luminous sensor is further explored. As shown in Figure 5a, the photoluminescence spectra of different pesticides ($\lambda_{\text{ex}} = 304 \text{ nm}$) were recorded separately. The quenching effect

of CP 1 on most pesticides was not obvious, and the quenching effect on Flu was the most obvious. In addition, Flu can be selectively tested under the interference of other pesticides. The fluorescence intensity did not decrease significantly when other pesticides were added, but the fluorescence was obviously quenched after the addition of Flu, as shown in Figure 5b. The experiment showed that CP 1 had a good selectivity to Flu.

To investigate the quenching effect of different concentrations of Flu (10 mmol/L) on CP 1 fluorescence at room temperature, quantitative experiments were conducted. The fluorescence intensity decreased gradually with the gradual increase in Flu concentration (10 mmol/L, 0 $\mu\text{mol/L}$ to 65 $\mu\text{mol/L}$). The fluorescence was almost completely quenched when the concentration was increased to 65 $\mu\text{mol/L}$, as shown in Figure 5c. In order to study the relationship between Flu concentration and fluorescence intensity more accurately, the linear curve was fitted according to the S–V equation. When the concentration increased to 65 μM , the linear relationship was good in the low concentration range of 2.0×10^{-5} to 5.5×10^{-5} : $Y = 3.9894 \times 10^5 X - 7.0826$ ($R^2 = 0.9941$). It was calculated that the detection limit reached 13.8 nM (Figure 5d).

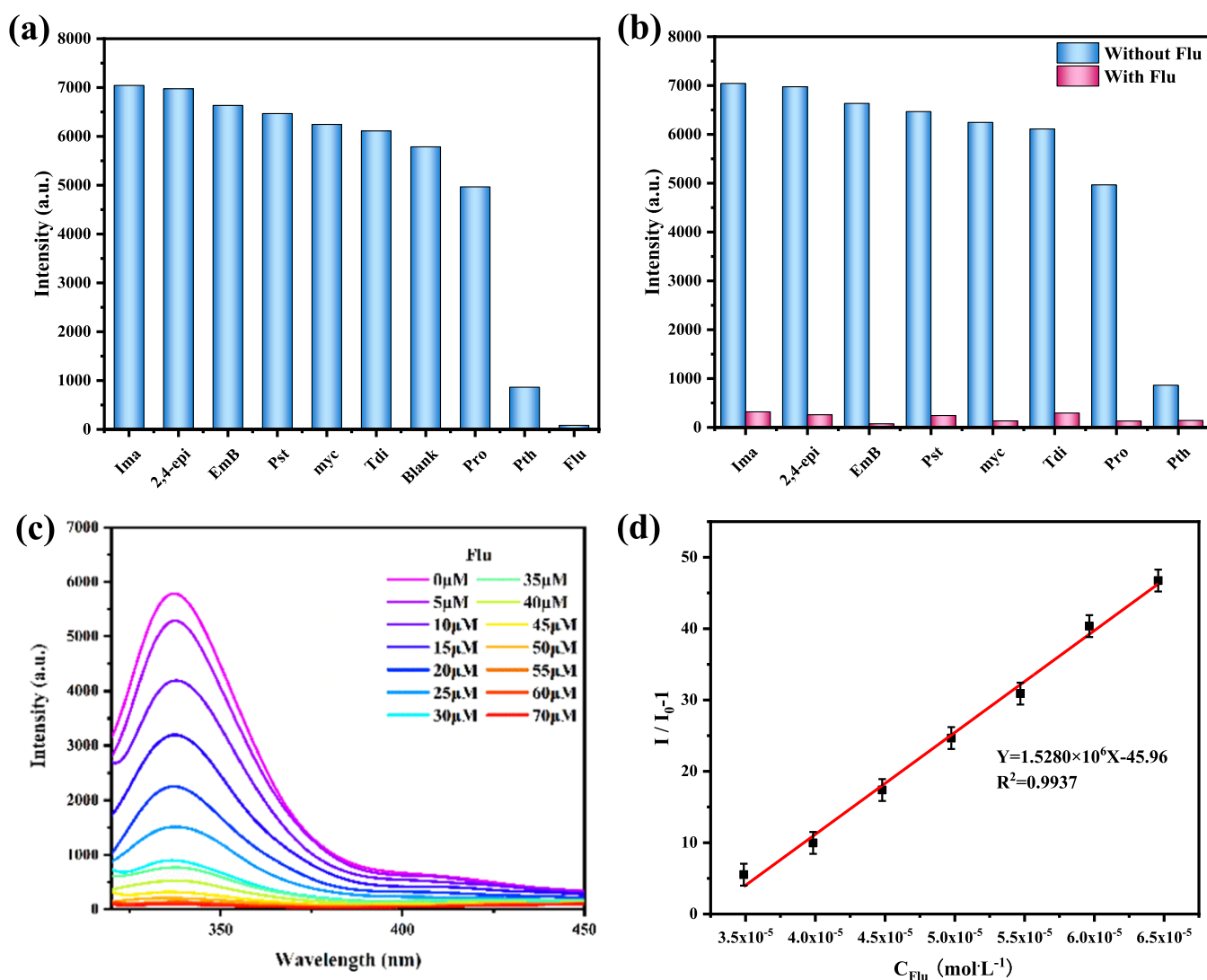


Figure 6. (a) Fluorescence intensity of CP 2 dispersed in different pesticides; (b) anti-interference experiment; (c) fluorescence emission spectrum of CP 2 with different concentrations of Flu; and (d) linear fitting curve.

When the excitation spectrum is 310 nm, the emission spectrum of CP 2 is 336 nm. The photoluminescence spectra of different pesticides ($\lambda_{\text{ex}} = 310$ nm) are recorded, respectively. The test results showed that CP 2 had different quenching effects on different pesticides, among which Flu had the most obvious quenching effect, as shown in Figure 6a. Flu can be selectively tested under the interference of other pesticides. The fluorescence intensity did not decrease significantly when other pesticides were added, but the fluorescence was obviously quenched after the addition of Flu, as shown in Figure 6b. The anti-interference experiment showed that CP 2 had a good anti-interference ability to Flu without the influence of other selected pesticides after adding Flu.

To investigate the quenching effect of different concentrations of Flu (10 mmol/L) on CP 2 fluorescence at room temperature, the fluorescence intensity decreased gradually with the gradual increase in Flu concentration (10 mmol/L, 0–70 $\mu\text{mol/L}$). The fluorescence was almost completely quenched when the concentration increased to 70 $\mu\text{mol/L}$, as shown in Figure 6c. When the concentration increases to 70 μM , there is a good linear relationship in the low concentration range of 1.5×10^{-5} to 5.5×10^{-5} : $Y = 1.5280 \times 10^6 X - 45.96$ ($R^2 = 0.9937$);

the detection limit of Flu was estimated to be 52.7 nM (Figure 6d). The detection limit is lower than the reported value.⁴⁰

3.7. Discussion on the Quenching Mechanism. Detailed research was conducted on the sensing mechanisms of CP 1 on PNBA, Flu, and CP 2 on TNP and Flu. It is believed that the luminescence changes of metal organic complexes are mediated by the following factors: structural collapse, energy competitive absorption, resonance energy transfer, central metal ion exchange, and photoluminescence electron transfer (PET).⁴¹

The PXRD spectra generated by CP 1 dispersed in PNBA and Flu aqueous solutions are highly similar to the main peaks of the simulated spectra. The PXRD spectra generated by CP 2 dispersed in TNP and Flu aqueous solutions also showed good agreement with the simulated spectra, ruling out the possibility of skeleton collapse as the cause (Figure S2). Because CPs 1–2 detect nitro explosives and pesticides, they indicate that there is no metal ion exchange during fluorescence quenching. In addition, the overlapping area between the excitation emission spectra of the complex and the UV absorption spectra of the responsive compound was studied.^{42,43} The results indicate that the absorption spectra of nitro explosive PNBA and pesticide Flu overlap with the excitation spectra of CP 1 (Figure S4),

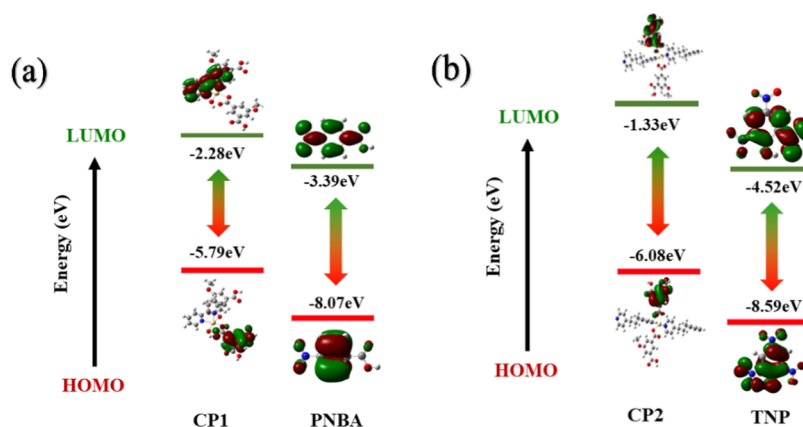


Figure 7. (a) HOMO and LUMO energies of CP 1 and nitro explosives. (b) HOMO and LUMO energies of CP 2 and nitro explosives.

suggesting that the quenching mechanism of both is energy competitive absorption. The emission spectrum of CP 2 overlaps significantly with the absorption spectrum of TNP (Figure S5a), and its quenching mechanism is resonance energy transfer. The absorption spectrum of Flu overlaps with the excitation spectrum of CP 2 (Figure S5b), suggesting that the quenching mechanism is energy competitive absorption. Therefore, the energy resonance transfer mechanism and energy competitive absorption mechanism are the factors that lead to fluorescence quenching.

On the other hand, density functional theory (DFT) calculations show that the LUMO energy level (-2.28 eV) of CP 1 is higher than those of PNBA (-3.39 eV) (Figure 7a) and Flu (-4.10 eV) (Figure 8), and the LUMO energy level (-1.33

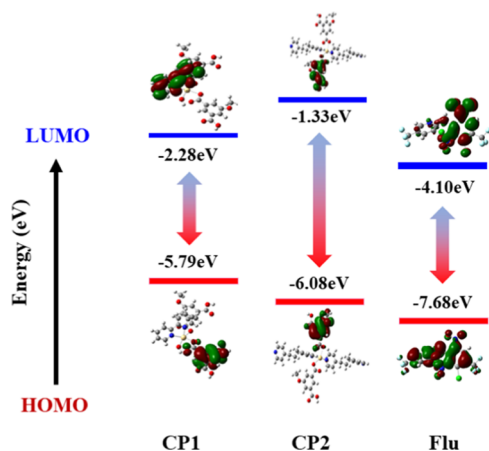


Figure 8. HOMO and LUMO energies of CP 1, CP 2, and pesticides.

eV) of CP 2 is higher than those of TNP (-4.52 eV) (Figure 7b) and Flu (-4.10 eV) (Figure 8). Therefore, during excitation, electrons are induced to transfer from the LUMO orbitals of CP 1 and CP 2 to the LUMO orbitals of the analyte. This leads to a fluorescence quenching effect.^{44–47} Therefore, we infer that the PET mechanism is also the cause of fluorescence quenching.

3.8. Detection of Flu in Yan River. Based on the results of the above fluorescence sensing experiment, it is concluded that CP 1 is most sensitive to the detection of Flu and the detection limit is the lowest. CP 1 is selected for the actual sample determination. With Yan River as the actual sample, Flu in the water sample was detected by the adding and recovering methods, and CP 1 was placed in the water sample for reaction,

and then its fluorescence was measured. Three concentrations of Flu (30, 40, 50 μM) were added to the water samples, and each group was repeated 5 times. The results are shown in Table 2,

Table 2. Recovery Results of Determination of CP 1-Flu in Real Samples ($n = 5$)

sample	content (μM)	added (μM)	detected (μM)	recovery (%)	RSD (%)
river 1	0	30.00	29.04	96.8	0.8
river 2		40.00	40.80	102.0	2.5
river 3		50.00	49.35	98.7	2.7

with recoveries ranging from 96.8 to 102.0%. The results show that CP 1 is one of the few complexes that can be used for the quantitative detection of Flu in actual samples and has certain feasibility for the quantitative detection of pesticides in water samples.

4. CONCLUSIONS

Two cadmium complexes with excellent fluorescence properties, CP 1 and CP 2, were synthesized by using the dicarboxylic acid ligand H_2zgt and different nitrogen-containing ligands. CP 1 had a quenching response to p-nitrobenzoic acid (PNBA) with a detection limit of 3.28 nM, while CP 2 had a quenching response to 2,4,6-trinitrophenol (TNP) with a detection limit of 11.4 nM. Both CP 1 and CP 2 were responsive to the pesticide fluridone (Flu). The detection limits were 13.8 and 52.7 nM. CP 1 has the lowest detection limit of Flu, and it is selected for the detection of actual water samples. The results show that CP 1 has a certain application prospect for the quantitative detection of Flu in actual water samples. Finally, the sensing mechanism is discussed in detail. The cause of PNBA/TNP and Flu quenching might be competitive absorption/energy resonance transfer or electron transfer.

ASSOCIATED CONTENT

Supporting Information

The Supporting Information is available free of charge at <https://pubs.acs.org/doi/10.1021/acsomega.3c06439>.

data_yd2180_a (CIF)

Structure factors have been supplied for datablock(s)

yd2180_a (PDF)

data_yd2200_a (CIF)

Structure factors have been supplied for datablock(s)

yd2200_a (PDF)

PXRD diagram of CPs 1–2; TGA pattern of CPs 1–2; solid fluorescence spectra of CPs 1–2; emission excitation spectrum of CPs 1–2; and ultraviolet absorption spectrum of analytes. Crystal data and structure refinement for CPs 1–2. Selected bond distances (nm) and bond angles ($^{\circ}$) for CPs 1–2. Hydrogen bond distances (nm) and bond angles (deg) for CP 1 (PDF)

AUTHOR INFORMATION

Corresponding Author

Hua-li Cui – Shaanxi Key Laboratory of Chemical Reaction Engineering, Laboratory of New Energy and New Function Materials, College of Chemistry and Chemical Engineering, Yan'an University, Yan'an 716000, P. R. China; orcid.org/0009-0006-9876-8377; Email: cuihuali07@163.com

Authors

Wen Liu – Shaanxi Key Laboratory of Chemical Reaction Engineering, Laboratory of New Energy and New Function Materials, College of Chemistry and Chemical Engineering, Yan'an University, Yan'an 716000, P. R. China; orcid.org/0000-0002-4161-0214

Xin-yue Xu – Shaanxi Key Laboratory of Chemical Reaction Engineering, Laboratory of New Energy and New Function Materials, College of Chemistry and Chemical Engineering, Yan'an University, Yan'an 716000, P. R. China

Jie Zhou – Shaanxi Key Laboratory of Chemical Reaction Engineering, Laboratory of New Energy and New Function Materials, College of Chemistry and Chemical Engineering, Yan'an University, Yan'an 716000, P. R. China

Xiao-ming Song – Shaanxi Key Laboratory of Chemical Reaction Engineering, Laboratory of New Energy and New Function Materials, College of Chemistry and Chemical Engineering, Yan'an University, Yan'an 716000, P. R. China

Xiao-li Chen – Shaanxi Key Laboratory of Chemical Reaction Engineering, Laboratory of New Energy and New Function Materials, College of Chemistry and Chemical Engineering, Yan'an University, Yan'an 716000, P. R. China

Complete contact information is available at:

<https://pubs.acs.org/10.1021/acsomega.3c06439>

Notes

The authors declare no competing financial interest.

ACKNOWLEDGMENTS

This work was supported by the National Natural Science Foundation of China (no. 21763028), the Science and Technology Project of Shaanxi Province (no. 2022QFY07-05 and 2022NY-071), the Science and Technology Project of Yan'an Province (no. 2022SLJBZ-002), and the Youth Innovation Team of Shaanxi Universities.

REFERENCES

- (1) Wang, M.; Jiang, L.; Yan, R.; Peng, M.; Huangfu, X.; Guo, Y.; Wu, P. Multifunctional luminescent Eu(III)-based metal-organic framework for sensing methanol and detection and adsorption of Fe(III) ions in aqueous solution. *Inorg. Chem.* **2016**, *55* (24), 12660–12668, DOI: [10.1021/acs.inorgchem.6b01815](https://doi.org/10.1021/acs.inorgchem.6b01815).
- (2) Zhang, X. Y.; Wang, K.; Chang, Y.; Hu, X. L.; Su, Z. M.; Zhou, E. L. Three Cd-MOFs with water stability act as novel fluorescent probes for detecting nitrofurantoin, nitrofurantoin and Fe³⁺. *J. Solid State Chem.* **2022**, *313*, 123170–123177.
- (3) Mi, X.; Sheng, D.; Yu, Y.; Wang, Y.; Zhao, L.; Lu, J.; Li, Y.; Li, D.; Dou, J.; Duan, J.; Wang, S. Tunable light emission and multiresponsive luminescent sensitivities in aqueous solutions of two series of lanthanide metal-organic frameworks based on structurally related ligands. *ACS Appl. Mater. Interfaces* **2019**, *11* (8), 7914–7926.
- (4) Kang, X. M.; Fan, X. Y.; Hao, P. Y.; Wang, W. M.; Zhao, B. A stable zinc-organic framework with luminescence detection of acetylacetone in aqueous solution. *Inorg. Chem. Front.* **2019**, *6* (1), 271–277.
- (5) Zhu, S. Y.; Yan, B. Highly sensitive luminescent probe of aniline and trace water in organic solvents based on covalently modified lanthanide metal-organic frameworks. *Ind. Eng. Chem. Res.* **2018**, *57* (49), 16564–16571.
- (6) Weng, H.; Yan, B. A flexible Tb(III) functionalized cadmium metal organic framework as fluorescent probe for highly selectively sensing ions and organic small molecules. *Sens. Actuators, B* **2016**, *228*, 702–708.
- (7) Yang, Q.; Wang, J.; Chen, X.; Yang, W.; Pei, H.; Hu, N.; Li, Z.; Suo, Y.; Li, T.; Wang, J. Simultaneously detection and removal of organophosphorus pesticide by a novel Zr-MOF based smart adsorbent. *J. Mater. Chem. A* **2018**, *6* (5), 2184–2192.
- (8) Sohrabi, H.; Sani, P. S.; Orooji, Y.; Majidi, M. R.; Yoon, Y.; Khataee, A. MOF-based sensor platforms for rapid detection of pesticides to maintain food quality and safety. *Food Chem. Toxicol.* **2022**, *165*, 113176–113180, DOI: [10.1016/j.fct.2022.113176](https://doi.org/10.1016/j.fct.2022.113176).
- (9) Wang, G. D.; Li, Y. Z.; Shi, W. J.; Zhang, B.; Hou, L.; Wang, Y. Y. A robust cluster-based Eu-MOF as multi-functional fluorescence sensor for detection of antibiotics and pesticides in water. *Sens. Actuators, B* **2021**, *331*, 129377–129386.
- (10) Fan, M. Y.; Sun, B.; Li, X.; Pan, Q. Q.; Sun, J.; Ma, P. F.; Su, Z. Highly Fluorescent Cadmium Based Metal–Organic Frameworks for Rapid Detection of Antibiotic Residues, Fe³⁺ and Cr₂O₇²⁻. *Ions Chem.* **2021**, *60* (12), 9148–9156, DOI: [10.1021/acs.inorgchem.1c01165](https://doi.org/10.1021/acs.inorgchem.1c01165).
- (11) Wang, G. D.; Li, Y. Z.; Shi, W. J.; Zhang, B.; Hou, L.; Wang, Y. Y. A robust cluster-based Eu-MOF as multi-functional fluorescence sensor for detection of antibiotics and pesticides in water. *Sens. Actuators, B* **2021**, *331* (15), 129377–129382.
- (12) Guo, J.; Han, X. D.; Wang, S.; Liu, M.; Liu, L. H.; Wang, P. A cucurbit[6]uril based supramolecular assembly for the detection and removal of dyes and antibiotics from water. *Anal. Methods* **2022**, *14* (26), 2642–2648.
- (13) Wei, J. H.; Yi, J. W.; Han, M. L.; Li, B.; Liu, S.; Wu, Y. P.; Ma, L. F.; Li, D. S. A water-stable terbium(III)-organic framework as a chemosensor for inorganic ions, nitro-containing compounds and antibiotics in aqueous solutions. *Chem. - Asian J.* **2019**, *14* (20), 3694–3701.
- (14) Xing, S.; Bing, Q.; Qi, H.; Liu, J.; Bai, T.; Li, G.; Shi, Z.; Feng, S.; Xu, R. Rational design and functionalization of a zinc metal-organic framework for highly selective detection of 2,4,6-trinitrophenol. *ACS Appl. Mater. Interfaces* **2017**, *9* (28), 23828–23835.
- (15) Zhao, P.; Liu, Y.; He, C.; Duan, C. Synthesis of a lanthanide metal-organic framework and its fluorescent detection for phosphate group-based molecules such as adenosine triphosphate. *Inorg. Chem.* **2022**, *61* (7), 3132–3140.
- (16) Huang, L.; Cheng, H.; Wang, L.; Wu, X.; Qin, B. Anion exchange on surface induces drastic fluorescence response in Cu(II) coordination polymer crystals. *Cryst. Growth Des.* **2021**, *21* (4), 1905–1911.
- (17) Wang, Y.; Zhou, Y. N.; Liang, Y.; Cheng, L.; Fang, Y. Chiral fluorescent metal-organic framework with a pentanuclear copper cluster as an efficient luminescent probe for Dy³⁺ ion and cyano compounds. *Inorg. Chem.* **2021**, *60* (20), 15085–15090.
- (18) Guan, Q. L.; Sun, Y.; Huo, R.; Xin, Y.; Bai, F. Y.; Xing, Y. H.; Sun, L. X. Cu-MOF material constructed with a triazine polycarboxylate skeleton: multifunctional identify and microdetecting of the aromatic diamine family (o, m, p-phenylenediamine) based on the luminescent response. *Inorg. Chem.* **2021**, *60* (4), 2829–2838.
- (19) Wang, Y. L.; Li, X. Y.; Han, S. D.; Pan, J.; Xue, Z. Z. A Cu₂I₂-based coordination framework as the selective sensor for Ag⁺ and the effective adsorbent for I₂. *Cryst. Growth Des.* **2022**, *22* (6), 3719–3726.

- (20) Jiang, Q. J.; Lin, J. Y.; Hu, Z. J.; Hsiao, V. K. S.; Chung, M. Y.; Wu, J. Y. Luminescent zinc(II) coordination polymers of bis(pyridin-4-yl)benzothiadiazole and aromatic polycarboxylates for highly selective detection of Fe(III) and high-valent oxyanions. *Cryst. Growth Des.* **2021**, *21* (4), 2056–2067.
- (21) Mendiratta, S.; Tseng, T. W.; Luo, T. T.; Luo, T. T.; Chen, C.; Huang, C. Y. Differentially activated amino acid coordination polymers by amino acids. *Cryst. Growth Des.* **2018**, *18* (5), 2672–2676, DOI: 10.1021/acs.cgd.8b00012.
- (22) Han, Z.; Wang, K.; Zhou, H. C.; et al. Preparation and quantitative analysis of multicolor luminescence materials for sensing function. *Nat. Protoc.* **2023**, *18*, 1621–1640.
- (23) Han, Z.; Wang, K.; Chen, Y.; Li, J.; Teat, S. J.; Yang, S.; Cheng, P. A multicenter metal–organic framework for quantitative detection of multicomponent organic mixtures. *CCS Chem.* **2022**, *4* (10), 3238–3245, DOI: 10.31635/ccschem.022.202101642.
- (24) Xi, X.; Liu, Y.; Cui, Y. Homochiral silver-based coordination polymers exhibiting temperature-dependent photoluminescence behavior. *Inorg. Chem.* **2014**, *53* (5), 2352–2354.
- (25) Boer, S. A.; Turner, D. R. Interpenetration in π -Rich mixed-ligand coordination polymers. *Cryst. Growth Des.* **2016**, *16* (11), 6294–6303.
- (26) Liu, H.; Wang, Y.; Qin, Z.; Liu, D.; Xu, H.; Dong, H.; Hu, W. Electrically conductive coordination polymers for electronic and optoelectronic device applications. *J. Phys. Chem. Lett.* **2021**, *12* (6), 1612–1630.
- (27) Wen, Y.; Feng, M.; Zhang, P.; Zhou, H. C.; Sharma, V. K.; Ma, X. Metal organic frameworks (MOFs) as photocatalysts for the degradation of agricultural pollutants in water. *ACS ES&T Engg* **2021**, *1* (5), 804–826.
- (28) Liu, Y.; Tang, C.; Cheng, M.; Chen, M.; Chen, S.; Lei, L.; Chen, Y.; Yi, H.; Fu, Y.; Li, L. Polyoxometalate@metal-organic framework composites as effective photocatalysts. *ACS Catal.* **2021**, *11* (21), 13374–13396.
- (29) Chen, C.; Zhang, H. D.; Tao, Y.; Liang, L. J.; He, C.; Su, B. C.; Li, H. Y.; Huang, F. P. Tracking the stepwise formation of a water-soluble fluorescent Tb₁₂ cluster for efficient doxorubicin detection. *Inorg. Chem.* **2022**, *61* (25), 9385–9391.
- (30) Bairy, G.; Dey, A.; Dutta, B.; Ray, P. P.; Sinha, C. 2D Cd(II)-MOF of pyridyl-imidazoquinazoline: structure, luminescence, and selective detection of TNP and fabrication of semiconducting devices. *Cryst. Growth Des.* **2022**, *22* (5), 3138–3147.
- (31) Guo, C. L.; Yan, Li.; Jie, C.; Na, Xu.; Xiu, L. W.; Hong, Y. L.; Bao, K. C.; Jian, R. L. Various Cd(II) coordination polymers induced by carboxylates: multi-functional detection of Fe³⁺, anions, aspartic acids and bovine serum albumin. *Dalton Trans.* **2020**, *49* (3), 737–740, DOI: 10.1039/C9DT04103F.
- (32) Li, X. J.; Guang, C. M.; Xia, H. X. Syntheses, structures, and properties of two coordination polymers based on 5-methoxyisophthalate and flexible dipyridines. *J. Coord. Chem.* **2013**, *16* (18), 3249–3260, DOI: 10.1080/00958972.2013.832759.
- (33) Gcwensa, N.; Oliver, C. L. Large Differences in Carbon Dioxide and Water Sorption Capabilities in a System of Closely Related Isorecticular Cd (II)-based Mixed-Ligand Metal–Organic Frameworks. *Inorg. Chem.* **2020**, *59* (18), 13211–13222, DOI: 10.1021/acs.inorgchem.0c01533.
- (34) Wang, G. D.; Li, Y. Z.; Shi, W. J.; Zhang, B.; Hou, L.; Wang, Y. Y. A robust cluster-based Eu-MOF as multi-functional fluorescence sensor for detection of antibiotics and pesticides in water. *Sens. Actuators, B* **2021**, *331*, 129377–129381.
- (35) Liu, C. H.; Guan, Q. L.; Yang, X. D.; Bai, F. Y.; Sun, L. X.; Xing, Y. H. Polyiodine-modified 1,3,5-benzenetricarboxylic acid framework Zn(II)/Cd(II) complexes as highly selective fluorescence sensors for thiamine hydrochloride, NACs, and Fe³⁺/Zn²⁺. *Inorg. Chem.* **2020**, *59* (12), 8081–8098.
- (36) Badiane, I.; Freslon, S.; Suffren, Y.; Daignebonne, C.; Calvez, G.; Bernot, K.; Camara, M.; Guillou, O. High Brightness and Easy Color Modulation in Lanthanide-Based Coordination Polymers with 5-Methoxyisophthalate as Ligand: Toward Emission Colors Additive Strategy. *Cryst. Growth Des.* **2017**, *17* (3), 1224–1234.
- (37) Gogoi, C.; Biswas, S. Aqueous-phase nanomolar detection of dichromate by a recyclable Cd(II) metal-organic framework. *Cryst. Growth Des.* **2021**, *21* (5), 2680–2689.
- (38) Hazra, A.; Bej, S.; Mondal, A.; Murmu, N. C.; Banerjee, P. Discerning detection of mutagenic biopollutant TNP from water and soil samples with transition metal-containing luminescence metal-organic frameworks. *ACS Omega* **2020**, *5* (26), 15949–15961.
- (39) Wang, X.; Hou, J.; Lan, S.; Shen, C.; Huo, D.; Ji, Z.; Ma, Y.; Luo, H.; Zhang, S.; He, Q.; Hou, C. MoS₂ QDs-Based sensor for measurement of fluazinam with triple signal output. *Anal. Chim. Acta* **2020**, *1108*, 152–159.
- (40) Wang, H. H.; Zhang, Y.; Yang, D. B.; Hou, L.; Li, Z. Y.; Wang, Y. Y. Fluorine-substituted regulation in two comparable isostructural Cd(II) coordination polymers: enhanced fluorescence detection for tetracyclines in water. *Cryst. Growth Des.* **2021**, *21* (4), 2488–2497.
- (41) Baikeli, Y.; Mamat, X.; Chen, L. F.; Liu, X. S.; Shen, L.; Lyu, Y. Q.; Li, C. H. Ultrasensitive and simultaneous determination of p-Nitrophenol and p-Nitrobenzoic acid by a modified glassy carbon electrode with N-rich nanoporous carbon derived from ZIF-8. *J. Electroanal. Chem.* **2021**, *899*, 115567–115569.
- (42) Rachuri, Y.; Parmar, B.; Suresh, E. Three dimensional Co (II)/Cd (II) MOFs: luminescent Cd-MOF for detection and adsorption of TNP in aqueous phase. *Cryst. Growth Des.* **2018**, *18* (5), 3062–3072.
- (43) Guo, C. L.; Yan, Li.; Jie, C.; Na, Xu.; Xiu, L. W.; Hong, Y. L.; Yong, Q. C. Multi-functional fluorescent responses of Cobalt complexes derived from functionalized amide-bridged ligand. *Dyes Pigm.* **2020**, *174*, 108064–108069, DOI: 10.1016/j.dye-pig.2019.108064.
- (44) Bairy, G.; Dey, A.; Dutta, B.; Ray, P. P.; Sinha, C. 2D Cd(II)-MOF of pyridyl-imidazoquinazoline: structure, luminescence, and selective detection of TNP and fabrication of semiconducting devices. *Cryst. Growth Des.* **2022**, *22* (5), 3138–3147.
- (45) Guo, Y. Y.; Shi, S. X.; Fan, C. Y.; Jin, D. Fluorescent determination of fluazinam with polyethyleneimine-capped copper nanoclusters. *Chem. Phys. Lett.* **2020**, *754*, 137748–137754.
- (46) Zhao, Y.; Zeng, H.; Zhu, X. W.; Lu, W.; Li, D. Metal–organic frameworks as photoluminescent biosensing platforms: mechanisms and applications. *Chem. Soc. Rev.* **2021**, *50*, 4484–4513.
- (47) Liu, W.; Cui, H. L.; Zhou, J.; Su, Z. T.; Zhang, Y. Z.; Chen, X. L.; Yue, E. L. Synthesis of a Cd-MOF Fluorescence Sensor and Its Detection of Fe³⁺, Fluazinam, TNP, and Sulfasalazine Enteric-Coated Tablets in Aqueous Solution. *ACS Omega* **2023**, *8* (27), 24635–24643.